



## Periodicities in mid- to late-Holocene peatland hydrology identified from Swedish and Lithuanian tree-ring data



Johannes Edvardsson<sup>a, b, \*</sup>, Florian Adolphi<sup>b</sup>, Hans W. Linderholm<sup>c</sup>, Christophe Corona<sup>d</sup>, Raimund Muscheler<sup>b</sup>, Markus Stoffel<sup>a, e, f</sup>

<sup>a</sup> Dendrolab.ch, Institute of Geological Sciences, University of Bern, Baltzerstrasse 1+3, CH-3012 Bern, Switzerland

<sup>b</sup> Quaternary Sciences, Department of Geology, Lund University Sölvegatan 12, SE-223 62 Lund, Sweden

<sup>c</sup> Department of Earth Sciences, University of Gothenburg, Box 460, 405 30 Gothenburg, Sweden

<sup>d</sup> GEOLAB, UMR6042 CNRS and Blaise Pascal University, Maison des Sciences de l'Homme 4, Rue Ledru, F63057 Clermont-Ferrand Cedex 2, France

<sup>e</sup> Climatic Change and Climate Impacts, Institute for Environmental Sciences, University of Geneva, Boulevard Carl-Vogt 66, CH-1205 Geneva, Switzerland

<sup>f</sup> Department of Earth Sciences, University of Geneva, Rue des Maraîchers 13, CH-1205 Geneva, Switzerland

### ARTICLE INFO

#### Article history:

Received 24 December 2015

Received in revised form

16 February 2016

Accepted 17 February 2016

Available online xxx

#### Keywords:

Wavelet analysis

Spectral analysis

NAO

AMO

Solar variability

Lunar nodal tides

Sweden

Lithuania

### ABSTRACT

Twenty-five tree-ring width (TRW) chronologies, developed from moisture sensitive peatland trees in Sweden and Lithuania, and representing eight periods during the mid-Holocene to present, were analysed regarding common periodicities (cycles). Periods of 13–15, 20–22, and 30–35 years were found in most chronologies, while 8–10, 18–19, and 60–65 year periodicities were observed as well, but less commonly. Similar periodicities, especially about 15 and 30 years in duration, were detected in both living and subfossil trees, indicating that the trees have responded to similar forcing mechanisms on those timescales through time. Some of the detected periods may be related to solar variability and lunar nodal tides, but most of the detected periodicities are more likely linked to hydrological changes in the peatlands associated to atmospheric patterns such as the North Atlantic Oscillation (NAO), or variations in sea surface temperatures (i.e. the Atlantic Multidecadal Oscillation, AMO). However, no significant relationships between tree growth, NAO and AMO could be formally established, possibly due to hydrological lag and feedback effects which are typical for peatlands but render in-depth assessments rather difficult.

© 2016 Elsevier Ltd. All rights reserved.

## 1. Introduction

The impact of climate change on ecosystems is a key issue for society requiring advanced knowledge about climate variability and its forcing mechanisms (Moss et al., 2010). In recent decades, improved palaeoclimatic methods have enabled more robust climate reconstructions (Wanner et al., 2008; Marcott et al., 2013; Stoffel et al., 2015), but there is still a critical need for proxy data providing precise and detailed information about long-term moisture variability (Wu et al., 2002; Edvardsson et al., 2016). Annual growth rings from peatland trees have proven to reflect moisture variability over both the recent past (Linderholm et al., 2002; Edvardsson et al., 2015) and the Holocene (Pilcher et al.,

1984; Leuschner et al., 2002). Long distance cross-correlations between peatland tree-ring width (TRW) chronologies from different geographical settings suggest that common large-scale climate forcing often influenced tree growth (Leuschner et al., 2002; Edvardsson et al., 2012a). TRW data from peatland trees will, however, remain an underutilized source of long-term climate and environmental information for as long as the exact linkage between peatland tree growth, hydrology, and large-scale climate dynamics is not sufficiently understood. To access the full potential of data series obtained from peatland trees, further studies comparing tree growth to various climate proxies are critically needed, as are comparative studies between different geographical regions and periods of the Holocene.

Changes in solar activity (Babcock, 1961; Muscheler et al., 2007), the heat distribution between the ocean and the atmosphere (Justino and Peltier, 2005), the North Atlantic Oscillation (NAO; van Loon and Rodgers, 1978; Hurrell, 1995) and the Atlantic Multidecadal Oscillation (AMO; Keer, 2000; Sutton and Dong, 2012) have

\* Corresponding author. Dendrolab.ch, Institute of Geological Sciences, University of Bern, Baltzerstrasse 1+3, CH-3012 Bern, Switzerland.

E-mail address: [johannes.edvardsson@dendrolab.ch](mailto:johannes.edvardsson@dendrolab.ch) (J. Edvardsson).

been shown to influence regional climate, but have been discussed to partly vary in a periodic (cyclic) or quasi-periodic manner which can be detected by frequency analyses. In this sense, the AMO has often been described as the observed pattern of multidecadal variations in North Atlantic sea surface temperatures (SSTs; Keer, 2000; Sutton and Dong, 2012), whereas the NAO is commonly defined as the leading mode of sea level pressure over the North Atlantic region (Hurrell et al., 2001); both oscillations are known to influence temperature and precipitation variability around the North Atlantic. As the moisture balance in peatlands depends on both precipitation and temperature-controlled evapotranspiration (Charman et al., 2009), tree growth in peatland ecosystems may reflect both local hydrology and regional climate variability (Edvardsson et al., 2015). Periodicities related to phenomena influencing the moisture status in peatlands are therefore likely to be traceable in annual growth patterns of peatland trees. Analysis of periodicities in TRW chronologies with different temporal and geographic distribution may thereby also be useful for the investigation of spatio-temporal hydroclimate variability.

To advance our knowledge about linkages between peatland tree growth and climate variability, TRW chronologies developed from Swedish and Lithuanian peatland trees were subjected to spectral and wavelet analyses. Fourier and wavelet transform spectral analyses (Jenkins and Watts, 1968; Torrence and Compo, 1998) were used to study periodicities in peatland tree growth. The Fourier transform spectra assess the power of a given frequency over an entire record and, thus, require a certain stability of the periodicities over time, whereas the wavelet power spectra allow for an investigation of non-persistent periodicities, i.e. they resolve the power of a given frequency at a given point in time (Torrence and Compo, 1998; Stoica and Moses, 2005).

Using the two different approaches, this paper therefore aims at (i) identifying potential periodicities (cycles) in the annual growth patterns of peatland trees, (ii) studying the spatial and temporal patterns of these periodic changes, and at (iii) discussing their potential origin.

## 2. Material and methods

### 2.1. Treatment of tree-ring width data

In total, 25 TRW chronologies from 11 Swedish and 5 Lithuanian peatlands were analysed for the purpose of this study (Table 1, Fig. 1). TRW chronologies were developed from 834 trees, covering about 4700 years separated into eight non-overlapping periods during the mid- and late-Holocene (Fig. 2). Apart from three oak chronologies (*Quercus robur* L.), the material consisted exclusively of Scots pine (*Pinus sylvestris* L.). The subfossil material originated from peatlands used for peat mining, whereas the living trees were sampled at raised bogs showing limited evidence of human activities. Accuracy of the cross-dating and TRW measurements were evaluated using the COFECHA software (Holmes, 1983). To minimize the influence of non-climatic variations and trends related to, for example, height within the stem and age, the TRW series from the individual trees were standardized and transformed into dimensionless indices (Fritts, 1976) before being averaged into chronologies. As the trees often showed growth trends with narrow rings during both juvenile and adolescent stages—as opposed to the negative exponential trend commonly observed in TRW series—various flexible standardization methods based on spline functions (Cook and Peters, 1981) or the Friedman variable span smoother (Friedman, 1984) were compared to make sure that detected periodicities were not artefacts from or lost in the standardization process. To highlight high- and low-frequency patterns in the data series respectively, the standardizations were also

performed using different bandwidths. A short bandwidth keeps the high-frequency variability in the data series whereas increasing bandwidth preserves low-frequency variations better (Esper et al., 2009). To assess the reliability of the TRW chronologies, we calculated the expressed population signal (EPS), a parameter that is dependent on the number of overlapping series and their mutual conformity. The limit at which the TRW chronologies were considered to be reliable and well replicated was set to the commonly applied threshold of  $EPS \geq 0.85$  (Wigley et al., 1984). Both standardization and calculation of EPS values were performed using the ARSTAN\_41d software (Cook and Krusic, 2006).

### 2.2. Analyses of the tree-ring width data

The spectral frequencies were calculated using Fourier frequency spectra with the Tukey-Hanning window (Blackman and Tukey, 1958). To evaluate the spectra further and to test the significance of detected spectral peaks, we used the multi-taper method (Thomson, 1982; Rögnvaldsson, 1993). Detected periodicities were separated depending on their significance levels ( $p < 0.001$ ,  $p < 0.01$  or  $p < 0.05$ ), whereas remaining periodicities ( $p > 0.05$ ) were excluded from further analyses. Wavelet analysis was performed to visualize the temporal stability of detected periodicities over the entire time-span of each TRW chronology. The wavelet power spectrum was calculated and visualized using contour levels equal to 75%, 50%, 25%, and 5% of the normalized wavelet power, respectively. Significance levels were calculated using a red-noise (autoregressive lag1) background spectrum (Torrence and Compo, 1998) and periods showing wavelet power corresponding to significance level  $p < 0.05$  were highlighted. Analyses were made using the AutoSignal v1.7 software ([www.sigmaplot.com](http://www.sigmaplot.com)) and tools provided by the University of Colorado (Torrence and Compo, 1998). Four data series developed from subfossil trees did not pass the EPS threshold  $>0.85$  for extended periods (Table 1). In order not to exclude these data series completely, analyses were performed over the entire length of the TRW chronologies and for periods representing EPS values  $> 0.85$  separately. Results from those periods considered reliable ( $EPS > 0.85$ ) were considered for the results and discussion, whereas the analyses of the complete chronologies was considered as a valuable addition.

To study common tree growth responses among the TRW chronologies, cluster analyses (CA) were conducted on all chronologies from living trees. Chronologies falling into common clusters were thereafter stacked and compared to meteorological variables from the 20th century reanalysis project (version V2c, Compo et al., 2011) and the reconstructed sea surface temperatures (SSTs) from the HadISST dataset (Rayner et al., 2003). In addition, we tested if similar periodicities between TRW chronologies and well-known climate indices such as the NAO and AMO could be found using wavelet coherence analysis (Grinsted et al., 2004). Hydroclimatic conditions prior to and during the growth season of the trees have been found to influence the radial growth of peatland trees from both Sweden (Linderholm et al., 2002; Edvardsson and Hansson, 2015) and Lithuania (Edvardsson et al., 2015). Comparisons between clustered TRW chronologies and climatic variables were therefore performed using monthly pre-growth season (January to April; or JFMA) as well as main growth season (June to August; or JJA) data individually.

### 2.3. Results and their implications

Close to identical spectral frequency peaks and significance values were obtained in the initial tests with the Tukey-Hanning (Blackman and Tukey, 1958) and Multi-taper (Thomson, 1982; Rögnvaldsson, 1993) window methods, and regardless of the

**Table 1**  
Information about the TRW chronologies used for spectral and wavelet analyses. The table shows abbreviated site name, chronology code, tree species, number of trees used, length of the chronologies, the period each chronology covers, the period with EPS above 0.85, and previous publications (1 = Edvardsson et al., 2012a, 2 = Edvardsson et al., 2012b, 3 = Edvardsson, 2013, 4 = Edvardsson et al., 2014, 5 = Linderholm et al., 2002, 6 = Edvardsson and Hansson, 2015, 7 = Edvardsson et al., 2015, 8 = Edvardsson et al., 2016, and U = Edvardsson (unpublished data).

Site (Coordinates)	Code/Species	Trees (n)/Length (years)	Total period/EPS > 0.85 period	Previously presented
Subfossil material (Ages are BC if not AD ages shown)				
Åbumossen (56°19'N, 13°55'E)	AP1/Pine	159/1560	2668–1108/2480–1150	3
Aukstumala (55°23'N, 21°22' E)	AuP1/Pine	9/168	869–702 ± 72 <sup>a</sup> /–	8
Hällaryds M. (57°20'N, 14°35'E)	HP1/Pine	117/1112	4839–3728/4730–3830	1
Rëkyva (55°51'N, 23°15'E)	RP1/Pine	21/322	3610–3289 ± 55 <sup>a</sup> /3495–3297 ± 55 <sup>a</sup>	8
Rëkyva (55°51'N, 23°15'E)	RP2/Pine	6/234	1678–1445 ± 46 <sup>a</sup> /1555–1535 ± 46 <sup>a</sup>	8
Rieznycia (54°27'N, 24°32'E)	RP1/Pine	62/321	635–955 CE ± 36 <sup>a</sup> /666–899 ± 36 <sup>a</sup>	8
Viss Mosse (55°51'N, 13°49'E)	VO1/Oak	15/326	1725–1399/1700–1460	4
Viss Mosse (55°51'N, 13°49'E)	VO2/Oak	2/242	5837–5596 ± 66 <sup>a</sup> /–	4
Viss Mosse (55°51'N, 13°49'E)	VO3/Oak	3/292	5189–4898 ± 112 <sup>a</sup> /–	4
Viss Mosse (55°51'N, 13°49'E)	VP1/Pine	91/726	5284–4559/5220–4670	2 + 4
Viss Mosse (55°51'N, 13°49'E)	VP2/Pine	10/308	4236–3929/4200–4060	3
Viss Mosse (55°51'N, 13°49'E)	VP3/Pine	4/221	5467–5247 ± 74 <sup>a</sup> /–	2 + 4
Viss Mosse (55°51'N, 13°49'E)	VP4/Pine	7/186	6133–5948 ± 88 <sup>a</sup> /6070–6045 ± 88 <sup>a</sup>	2 + 4
Recent material (AD ages)				
Anebymossen (57°85'N, 14°63'E)	AnP1/Pine	21/118	1846–1996/1900–1996	5
Aukstumala (55°23'N, 21°22'E)	AuP2/Pine	24/127	1887–2013/1940–2013	7
Bredmossen (60°13'N, 16°08'E)	BrP1/Pine	21/191	1789–1996/1840–1996	5
Buxabygds M. (56°48'N, 14°13'E)	BP1/Pine	21/227	1785–2011/1925–2011	6
Čepkeliai (54°00'N; 24°30'E)	CP1/Pine	24/167	1848–2014/1860–2014	U
Fäjämyr (56°15'N, 13°33'E)	FP1/Pine	11/140	1872–2011/1935–2011	U
Hanvedsm. (59°13'N, 17°92'E)	HvP1/Pine	23/186	1800–1996/1830–1996	5
Hästhults M.(56°14'N, 13°29'E)	HaP1/Pine	25/144	1868–2011/1960–2011	6
Kerëplis (54°27'N, 24°32'E)	KP1/Pine	42/SS 207	1807–2013/1865–2013	7
Rëkyva (55°51'N, 23°15'E)	RP3/Pine	47/180	1843–2013/1905–2013	7
Saxnäs Mosse (56°51'N, 13°27'E)	SaP1/Pine	20/141	1871–2011/1915–2011	6
Store Mosse (57°14'N, 13°55'E)	SP1/Pine	49/163	1850–2012/1910–2012	6

<sup>a</sup> Uncertainty due to radiocarbon dating.

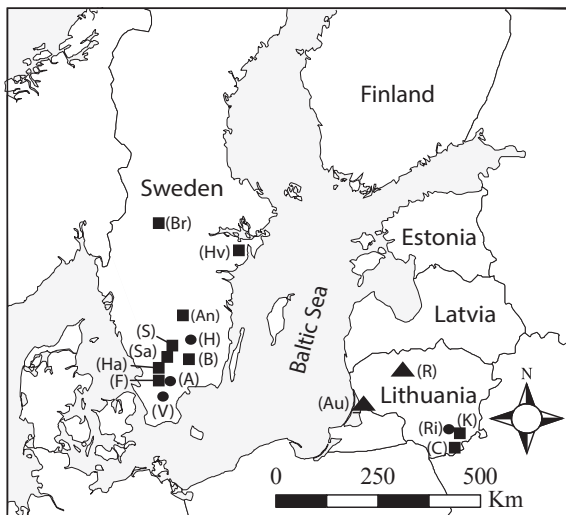


**Fig. 1.** Locations of the peatlands presented. The subfossil material (dots) originates from Åbumossen (A), Viss Mosse (V), Hällaryds mossen (H) and Rieznycia (Ri), whereas the contemporary material (squares) originate from Store Mosse (S), Anebymossen (An), Hanvedsmossen (Hv), Buxabygds Mosse (B), Bredmossen (Br), Fäjämyr (F), Hästhults Mosse (Ha), Saxnäs Mosse (Sa), Kerëplis (K) and Čepkeliai (C). Two sites, Rëkyva (R) and Aukstumala (Au), offered both subfossil and contemporary material (triangles).

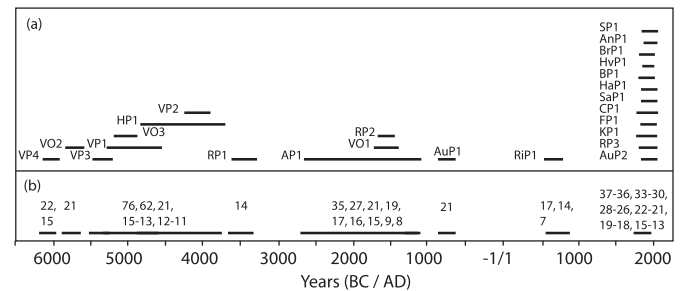


**Fig. 2.** (a) Temporal distribution of the TRW chronologies. (b) Periodicities (length in years) detected over each of the covered time periods.

based on analysis using the Tukey-Hanning window (Fig. 3) and standardized TRW chronologies to preserve low-frequency variations using Friedman's variable span smoother (Friedman, 1984).

#### 2.4. Spectral and wavelet analysis

From the spectral analysis, highly significant ( $p < 0.01$ ) to significant ( $p < 0.05$ ) frequency peaks were detected in all TRW chronologies except the Hästhults Mosse chronology (HaP1; Table 2) for which EPS values above 0.85 were only available after 1960, thus resulting in too few reliable years to analyse.

In the other chronologies, the most frequently occurring periodicities were those at 13–15, 20–22, and 30–35 years, but periodicities of c. 7–9, 11–12, 18–19, and 60–65 years were also encountered (Table 2; Fig. 4). The temporal stability of the periodicities was evaluated using wavelet analysis (Fig. 3). Most often, results from the wavelet analyses confirmed those from the spectral analyses, but some additional periodicities, on time scales shorter than 4 years in duration, were observed in five cases (i.e.,

standardization methods used. Comparison between TRW data using different standardization methods and meteorological data, however, showed best statistical results when we used a Friedman variable span smoother and bandwidth adjusted to preserve low-frequency variations (Edvardsson et al., 2015). Unless stated, all of the periodicities and significance levels henceforth presented were

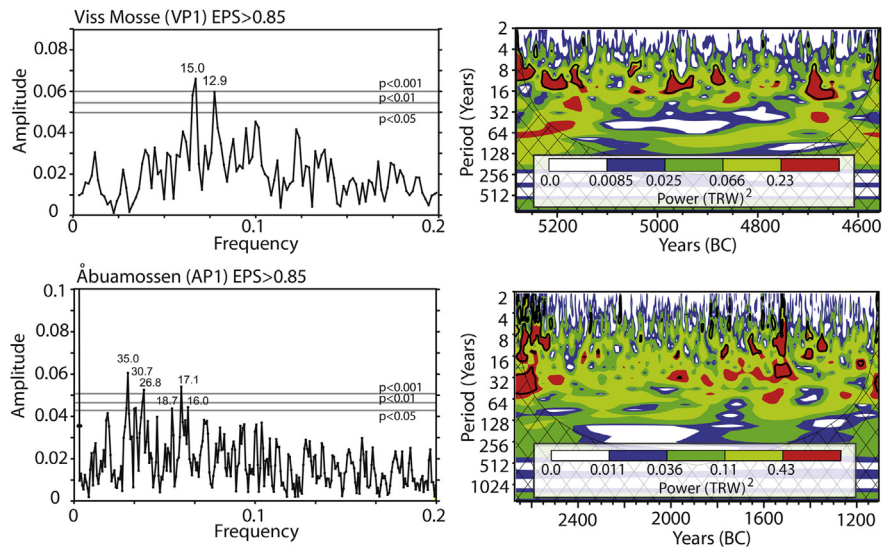


**Fig. 3.** The two examples show results from the spectral and wavelet analyses using the VP1 and AP1 TRW chronologies. To the left, power spectra using Tukey-Hanning window are shown. Periodicities in years are presented for peaks above the significance threshold of  $p < 0.05$ . To the right, wavelet power spectrum with contour levels of 75%, 50%, 25%, and 5% of the wavelet power are shown. For a complete overview of the results, see Table 2 and Fig. 4.

**Table 2**

Periodicities (length in years) detected based on spectral analysis using Fourier frequency spectra based on the Tukey-Hanning window for periods when TRW chronologies achieve  $EPS > 0.85$ . In brackets are periodicities detected when the whole TRW chronologies were analysed.

Code (Country)	Periodicities ( $p < 0.001$ )	Periodicities ( $p < 0.01$ )	Periodicities ( $p < 0.05$ )
<b>Subfossil material</b>			
AP1 (S)	35, 27, 17, (35, 17)	–	31, 19, 16, (27, 16)
AuP1 (L)	(21)	–	–
HP1 (S)	(62)	62	15, (9)
RP1 (L)	–	(14)	–
RP2 (L)	–	(21)	–
RiP1 (L)	–	(17)	14, (7)
VO1 (S)	(15, 9)	15, 9, (8)	8
VO2 (S)	–	(21)	–
VO3 (S)	–	–	(76, 13)
VP1 (S)	15	(15, 13)	–
VP2 (S)	–	12	(11)
VP3 (S)	–	(21)	–
VP4 (S)	–	–	(22, 15)
<b>Recent material</b>			
AnP1 (S)	–	(21)	30, (14)
AuP2 (L)	–	–	22
BrP1 (S)	26, (30)	–	(19)
BP1 (S)	(15)	(37)	–
CP1 (L)	28, (28)	–	–
FP1 (S)	–	(19)	–
HvP1 (S)	18, (18)	(30)	13, (13)
HaP1 (S)	–	–	–
KP1 (L)	33	14, (31)	–
RP3 (L)	–	28	(36, 26)
SP1 (S)	–	(15)	13
SaP1 (S)	–	(15)	–

AP1, BuP1, HaP1, RP2, and VP1). These short-term periodicities did, however, not appear as significant periodicities in any of the other analytical steps and were therefore not considered in further discussion. Some 7–9-year periodicities were detected in the subfossil material from both sides of the Baltic Sea (Table 2). Moreover, 13–15-year periodicities were frequently encountered, showing wide temporal and geographical distribution (Fig. 4). Periodicities of 18–19-years were, however, exclusively encountered in TRW chronologies developed from the Swedish material. Some 20–22-years periodicities were observed in seven TRW chronologies (Table 2, Fig. 4), but due to low sample replication several of these

chronologies did not reach  $EPS > 0.85$  for extended periods. Among the longer periodicities, which in this study correspond to those between 25 and 75 years in length, 30–35-year periodicities were most frequent and primarily observed in the living tree material (Table 2; Fig. 4).

2.5. Cluster analysis

To test if the periodicities with duration of c. 8–10, 20, and 50–70 years correspond to those described from various NAO and AMO records (Knight et al., 2005; Chylek et al., 2011; Olsen et al.,

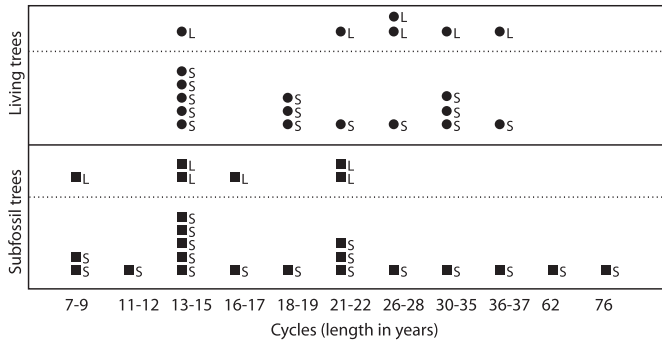


**Fig. 4.** Periodicities detected in TRW chronologies developed from subfossil (squares) and contemporary trees (circles) from Sweden (S) and Lithuania (L).

2012), wavelet coherency tests were performed using NAO (Jones et al., 1997; Luterbacher et al., 2002) as well as AMO records (van Oldenborgh et al., 2009). Some similar 20–25-year periodicities ( $p < 0.05$ ) between TRW and AMO were observed during first half of the 1900s for six of the analysed time series (AnP1, BrP1, BuP1, FP1, CeP1, and SaP1). Significant coherence at periodicities between 4 and 8 years were observed from the 1940s to 1970s between the AMO and five TRW chronologies (AuP2, BrP1, HvP1, RP1, and SP1). Periodicities of 8 to 16 years were observed in between the 1880s and 1920s for three chronologies (BuP1, HvP1, and KP1). But in general, no consistent or persistent common periodicities were revealed. Furthermore, the absolutely dated TRW chronologies developed from subfossil trees were compared to the  $^{14}\text{C}$ -production rate, which has been defined as a proxy for solar variability (Muscheler et al., 2005). Coherent periodicities between the records were, however, only detected around 32-years (VO1), 64-years (VP1), and 100–120-years (AP1, HP1), which are periodicities commonly not associated to solar variability.

From the Cluster Analysis (Fig. 5) three groups of chronologies; south-central Swedish (SCS), south Swedish (SS) and inland Lithuanian (L), were selected (Fig. 6) and compared to mean sea level pressure (MSLP) from the 20th century reanalysis data and SSTs from the HadISST dataset (Fig. 7). The majority of the test showed no clear relation, but the analysis using the SS-TRW cluster with SSTs reveal a spatial correlation pattern that bears similarities with

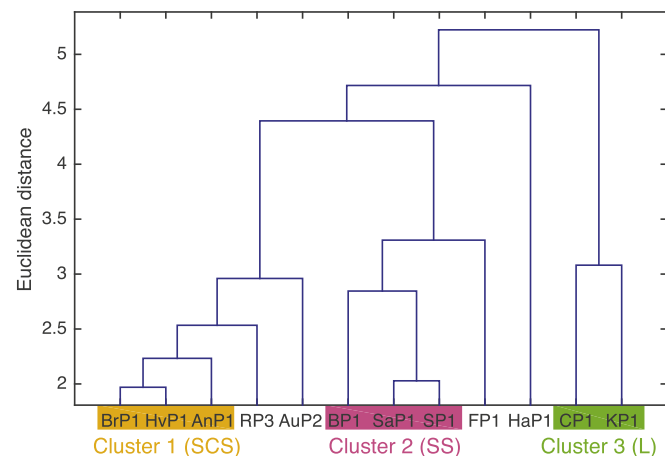


**Fig. 5.** Dendrogram of cluster analysis performed on the living TRW-chronologies. The clusters defined based on this analysis are highlighted in orange (Southern Central Sweden), pink (Southern Sweden) and green (Lithuania). (For interpretation of the references to colour in this figure legend, the reader is referred to the web version of this article.)

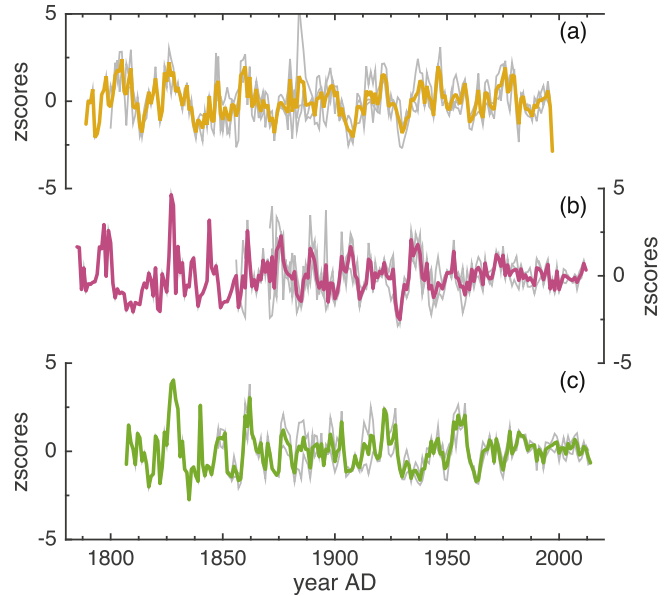


**Fig. 6.** Time series of the defined clusters. The individual TRW chronologies contributing to each cluster are shown in grey. Their mean, i.e., the cluster time series is shown as a coloured bold line. The colour coding is similar to Fig. 5. (a) Cluster 1 represent trees from Southern Central Sweden (SCS), (b), whereas cluster 2 represent Southern Sweden (SS), and (c) cluster 3 Lithuania (L). (For interpretation of the references to colour in this figure legend, the reader is referred to the web version of this article.)

the horseshoe pattern often associated with the AMO (Czaja and Frankignoul, 2002; Gastineau and Frankignoul, 2015, Fig. 7a). However, the obtained pattern is spatially more confined to the East Atlantic than the AMO pattern, and the TRW chronologies are not significantly correlated to the AMO index. Nevertheless, it appears that annual tree growth at the South Swedish peatlands is sensitive to pre-growing season SSTs in the East Atlantic, with enhanced growth during periods of low SSTs. The correlation between the SS and SCS cluster time-series and MSLP reveals a NAO/Arctic Oscillation-like correlation pattern during summer, but the correlation is for most regions only significant at 90–95% level (Fig. 7b–c).

### 3. Discussion

#### 3.1. Frequently recorded periodicities

Periodicities of 13–15, 20–22, and 30–35 years were frequently detected when peatland TRW chronologies were analysed from different geographical settings and covering different periods of the Holocene (Table 2; Fig. 4). From these observations, it can be concluded that some of the detected periodicities are likely associated with common responses to environmental forcing, and therefore probably linked to climate. The most frequently encountered 13–15-years periodicities are, for example, represented in 56% of the Swedish and 38% of the Lithuanian material (Fig. 4). Moreover, these periodicities were detected in both the pine and oak TRW chronologies, living trees and subfossil material, and were in several cases seemingly stable over time. Some 15-year periodicities were, for example, detected in trees growing at Viss Mosse around 5000 and 1600 BCE (VO1-VP1), and 14-year periodicities were observed in trees growing in the Rieznyca peatland at about 600 CE and the adjacent Kerėplis peatland under present climate conditions (RiP1-KP1). These results indicate that some coherent responses of annual tree growth were seemingly stable

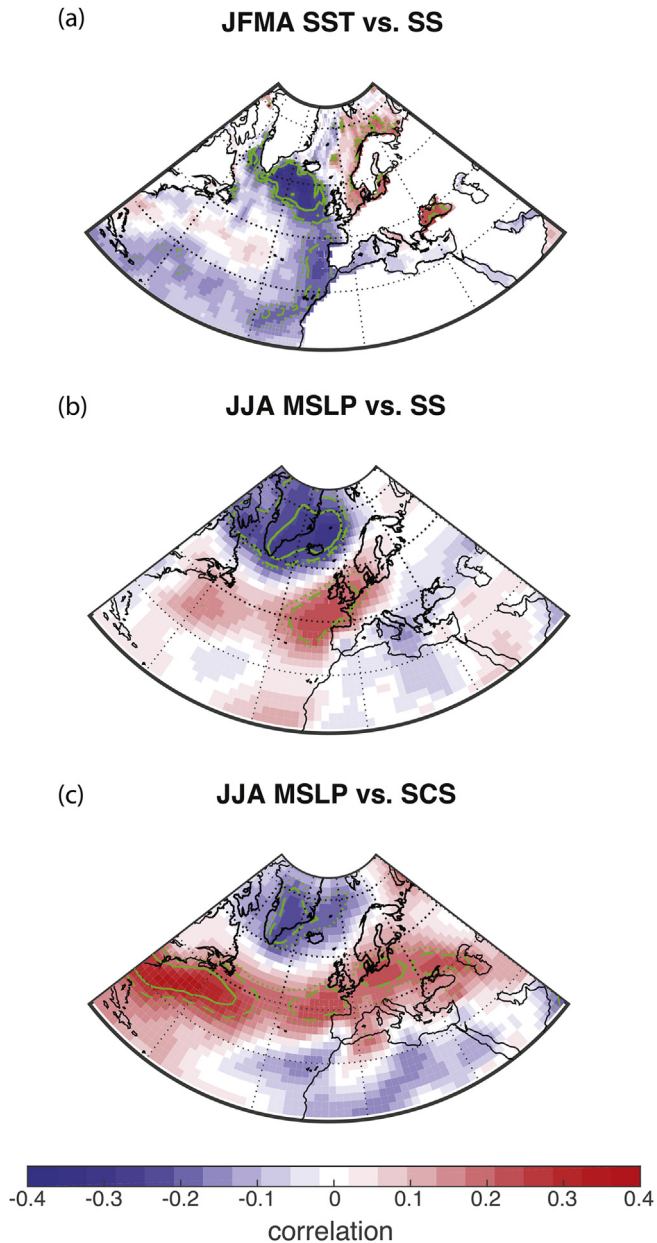


**Fig. 7.** (a) Correlation map of TRW-cluster 2 (SS) time series to pre-growth season (January–April) SSTs from the HadISST dataset (Rayner et al., 2003). (b) Correlation map of TRW-cluster 2 (SS) time series to growth season (June–August) mean sea level pressure from the 20th century reanalysis dataset (V2c, Compo et al., 2011). (c) Correlation map of TRW-cluster 1 (SCS) time series to June–August mean sea level pressure from the 20th century reanalysis dataset (V2c, Compo et al., 2011). Significant correlations are indicated by green dotted ( $p < 0.1$ ), dashed ( $p < 0.05$ ) and solid ( $p < 0.01$ ) contours. (For interpretation of the references to colour in this figure legend, the reader is referred to the web version of this article.)

throughout the mid- and late-Holocene. Also, the similarities in growth variability within the studied region suggest a common forcing, likely related to large-scale climate patterns. The existence of a common forcing has been postulated previously and in connection with the findings of long-distance correlations among peatland TRW chronologies from Ireland, Germany, and Sweden (Pilcher et al., 1984; Leuschner et al., 2002; Edvardsson et al., 2012a).

Precipitation and temperature-controlled evapotranspiration is usually governing the moisture status in peatlands (Charman et al.,

2009), and subsequently also growth conditions of trees (Boggie, 1972; Linderholm et al., 2002; Edvardsson et al., 2015). Periodicities related to large-scale oceanic and atmospheric patterns affecting the moisture regime over northwestern Europe should therefore have an imprint on TRW chronologies. The NAO is known to have a significant influence on the weather and climate dynamics in northwestern Europe (Hurrell et al., 2001; BACC, 2014), especially during winters. The prevailing conditions during winter and before the onset of the growth season have been shown to be of importance for the annual tree growth at both the Swedish and Lithuanian sites (Linderholm et al., 2002; Edvardsson et al., 2015). As the NAO influences precipitation patterns over northwest Europe (Loon and Rodgers, 1978; Olsen et al., 2012), it should logically affect the moisture status in Scandinavian and Baltic peatlands, and hence growth variability of moisture-sensitive peatland trees. Winters with a positive NAO index are usually associated with relatively wet conditions over Scandinavia (Greatbatch, 2000). Such NAO phases have been observed during the early 1900s, the 1920s, and since the 1980s (Hurrell et al., 2001), and would have generated moister conditions at most of the study sites. Reduced tree growth following positive NAO phases have been observed at several of the studied peatlands (Edvardsson et al., 2015; Edvardsson and Hansson, 2015), indicating a possible influence on tree growth, although significant year-to-year correlations are lacking in the data. Moreover, patterns similar to that of the summer NAO (Folland et al., 2009) can be observed in the correlation maps using stacked TRW data from the south Swedish sites (Fig. 7b–c), but cannot be seen in observational records so far.

The 13–15-year periodicities were frequently detected during the mid- and late-Holocene (Figs. 2 and 4). Several studies have described periodicities in North Atlantic SSTs of between 13 and 15 years (Sutton and Allen, 1997; Moron et al., 1998; Yndestad, 2006). Moreover, potential links between winter SSTs and radial tree growth in western Scandinavia have previously been discussed by Linderholm (2001). Thus, it can be assumed that the 13–15-year periodicities found in the TRW data reflects North Atlantic SST influences on the moisture regime in the studied region.

The periodicities of 30–35 years, which were observed in both the Swedish and Lithuanian material (Table 2; Fig. 4), have also been detected in TRW chronologies from the coast of Barents Sea (Raspopov et al., 2004) and northern Fennoscandia (Lindholm et al., 2011). Raspopov et al. (2004) suggested that the ~30-year periodicity was a manifestation of a combination of frequencies caused by nonlinear responses between different modes, whereas Justino and Peltier (2005) showed that simulated modern climate variability contains a 30-year periodicity associated with the AMO. Moreover, 30-year periodicities in the sea-level variability in the Finnish Gulf and Baltic Sea have been described and linked to the NAO in the past (Johansson et al., 2001).

Comparison of the SS TRW cluster with SSTs (Figs. 6–7) indicates a correlation pattern similar to the North Atlantic horseshoe pattern commonly associated with a negative phase of the AMO (Czaja and Frankignoul, 2002; Gastineau and Frankignoul, 2015). Over the 20th century, cold AMO phases occurred 1905–1925 and 1965–1990, whereas a warm phase has been recorded 1930–1960 (Sutton and Hodson, 2005; Knight et al., 2005). Warm AMO phases are often associated with an increase of precipitation in the low and high latitudes of the North Atlantic (Wei and Lohmann, 2012), and thereby moister conditions at our study sites. Depressed tree growth, indicating moist conditions, has been observed for extended periods from the 1930s to 1960s in peatland TRW chronologies from Lithuania (Edvardsson et al., 2015) and Sweden (Edvardsson and Hansson, 2015). By contrast, the opposite growth response is observed during the preceding AMO cold phase, c. 1905–1925 (Sutton and Hodson, 2005; Knight et al., 2005) for

which TRW data points to drier and more favourable growth conditions (Edvardsson et al., 2015). Combined, these observations indicate a possible connection between peatland tree growth and changes of NAO as well as AMO modes, although significant correlations were not obtained from the data. Nevertheless, it should be noted that peatlands should not be used as direct moisture recorders as they likely integrate regional moisture changes over time as a result of apparent hydrological lag and feedback effects (Kilian et al., 1995; Waddington et al., 2014) which may in turn blur short-term signals in TRW data. Dendroclimatological studies comparing annual tree growth at peatlands and meteorological data therefore show that the annual growth often reflects climate variability over periods of several years (Linderholm et al., 2002; Edvardsson et al., 2015; Edvardsson and Hansson, 2015), which renders a precise identification of NAO/AMO influences in TRW data more complex.

### 3.2. Less frequent periodicities

Periodicities of about 11 years length were observed in several TRW chronologies (Table 2; Fig. 4) resembling the solar 11-yr sunspot cycle. The Sun is the main energy source of the Earth and varies partly in a cyclic manner (Babcock, 1961; Damon and Peristykh, 2000; Muscheler et al., 2007). Several studies have demonstrated links between climate change and solar variability (Haigh, 2000; Bond et al., 2001; Adolphi et al., 2014), and linkages between solar variability and moisture balance in peatlands have been found by Mauquoy et al. (2004), Blaauw et al. (2004), and Mellström et al. (2015). Despite this, the wavelet coherence analyses between the  $^{14}\text{C}$ -production rate and tree growth did not show possible common variability for any periodicities commonly associated with solar changes (32-yr for VO1, 64-yr for VP1, and 100–120 yrs for AP1 and HP1) indicating that these records are not reflecting a direct climate influence of solar variability.

Periodicities of 18–19 years were exclusively encountered in the Swedish material (Table 2; Fig. 4). A 18.6-year periodicity related to the lunar nodal tide and linked to the declination of the moon has been described in several studies (O'Brien and Currie, 1993; Haigh et al., 2011). Although convincing evidence for the influence of a 18.6-year lunar nodal tide on climate has not been presented so far (Ray, 2006), periodicities of about 18.6 years have been detected in rainfall variations in India (Mitra et al., 1991), dryness-wetness indices from China (Currie, 1995), drought records in North America (Woodhouse et al., 1998), SSTs along the North American west coast (McKinnell and Crawford, 2007), as well as tree-ring data along the coast of the Barents Sea (Raspopov et al., 2004) and Scandinavia (Linderholm, 2001). Moreover, Yndestad et al. (2008) found correlations ( $r = 0.7$ ) between dominant Atlantic water temperature periodicities and the 18.6-year lunar nodal tide. This correlation, in combination with previously discussed observations of 18–19-year periodicities suggests that deterministic lunar nodal tides may indeed influence regional climate variability. Such an influence would naturally have an impact on moisture status in peatlands, at least in regions close to the Atlantic, which might in turn explain the presence of such periodicities in the Swedish material exclusively.

### 3.3. Comparison between contemporary and subfossil peatland trees

Relatively short periodicities, 7–11 years in duration, were exclusively encountered in the subfossil trees, whereas intermediate periodicities between 26 and 37 years were more frequently observed among the living material (Fig. 4). The organogenic layers beneath the trees have gradually grown thicker during the Holocene such that peat depths exceeding 6 m in thickness were

measured at several sites with a probe during field sampling of living trees. Increasing peat depth and peat volume are believed to generate more complex hydrological systems and possibly slower water-table responses, which in turn might be an explanation for the absence of short-term periodicities in the TRW chronologies developed from living trees. Several studies also indicate that peatland water-table fluctuations and associated tree growth may depend on total effective precipitation over several years (Linderholm et al., 2002; Edvardsson et al., 2015; Edvardsson and Hansson, 2015). By contrast, significantly shallower organogenic layers of 0.6–2 m were measured beneath the subfossil *in-situ* trees described by Edvardsson et al. (2012b; 2014). These relatively shallow peatlands were probably responding relatively quickly to hydrological variations, which would enable peatland trees growing during the mid-Holocene to capture rapid changes better than present trees. Slow hydrological responses in recent peatlands might therefore blur the climate signal in tree-ring data, decrease correlation between TRW and meteorological records, and cause difficulties in detection of short (<10 yrs) periodicities. In addition, the delayed and possibly integrated response of present peatlands to changes in atmospheric variability complicates a clear assessment of NAO/AMO related influences from peatland TRW records.

## 4. Conclusions

Periodicities of 13–15, 20–22, and 30–35 years were repeatedly encountered in TRW chronologies developed from both living and subfossil peatland trees. The periodicities were observed in different geographical settings and during various time periods, which likely points to large-scale similarities in the regional climate forcing from the mid-Holocene to the present time. The nature of these periodicities may, however, be subject to discussion, but are probably related to large-scale atmospheric circulation patterns such as the NAO, which exert an influence on precipitation and temperature around the southern Baltic Sea (BACC, 2014). Despite this, no significant correlations were obtained when our TRW chronologies were compared to NAO or AMO indices. Nevertheless, spatial correlation maps of TRW and MSLP or SSTs reveal patterns that bear similarities to those typically associated with the AMO and NAO, respectively (Fig. 7). The lack of correlation may therefore be related to hydrological lag effects in peatlands (Waddington et al., 2014; Edvardsson et al., 2015). The fact that peat depths has been much shallower with likely impacts on hydrological conditions and response times, we record short periodicities (<11 yrs) in the subfossil material. By contrast, and as a result of increasing peat depth and volume, short periodicities are absent in living trees and we mainly observe intermediate periodicities (25–40 yrs) under present-day conditions, due to the presence of a more complex hydrological systems and thereby slower water-table responses. Periodicities potentially corresponding to solar variability and lunar nodal tides were also detected, whereas other periodicities may be related to nonlinearity responses, or subsequent amplification between different periodicities causing combinatory frequencies.

Several studies have shown that common regional climate dynamics have influenced the annual growth of peatland trees, and that such TRW chronologies can be used as indicators for moisture variability and environmental changes during the Holocene (Pilcher et al., 1984; Leuschner et al., 2002; Edvardsson et al., 2012b). Our study strengthens the hypothesis that large-scale hydroclimatic forces have been governing peatland hydrology and associated tree growth as similar periodicities were detected during various periods as well as in different geographical settings. Simultaneously the interpretation of the results is difficult, which implies that continuous studies to understand how climate dynamics is affecting hydrology and tree growth in peatland

ecosystems are required.

## Acknowledgement

This study has been funded by the Lithuanian-Swiss cooperation program to reduce economic and social disparities within the enlarged European Union under the name CLIMPEAT (Climate change in peatlands: Holocene record, recent trends and related impacts on 394 biodiversity and sequestered carbon) project agreement No CH-3-SMM-01/05. We are grateful to Sébastien Guillet for support with software and two anonymous reviewers for valuable comments on the manuscript.

## References

- Adolphi, F., Muscheler, R., Svensson, A., Aldahan, A., Possnert, G., Beer, J., Sjolte, J., Björck, S., Matthes, K., Thiéblemont, R., 2014. Persistent link between solar activity and Greenland climate during the last glacial maximum. *Nat. Geosci.* 7 <http://dx.doi.org/10.1038/NGEO2225>.
- Babcock, H.W., 1961. The topology of the sun's magnetic field and the 22-year cycle. *Astrophys. J.* 133, 572–587.
- BACC Author Team, 2014. *Second Assessment of Climate Change for the Baltic Sea Basin*. Springer-Verlag, Berlin.
- Blackman, R.B., Tukey, J.W., 1958. *The Measurement of Power Spectra from the Point of View of Communication Engineering*. Dover Publications, p. 190.
- Blaauw, M., van Geel, B., van der Plicht, J., 2004. Solar forcing of climatic change during the mid-Holocene: indications from raised bogs in the Netherlands. *Holocene* 14, 35–44.
- Boggie, R., 1972. Effect of water-table height on root development of *Pinus contorta* on deep peat in Scotland. *Oikos* 23, 304–312.
- Bond, G., Kromer, B., Beer, J., Muscheler, R., Evans, M.N., Showers, W., Hoffmann, S., Lotti-Bond, R., Hajdas, I., Bonani, G., 2001. Persistent solar influence on north Atlantic climate during the Holocene. *Science* 294, 2130–2136.
- Charman, D.J., Barber, K.E., Blaauw, M., Langdon, P.G., Mauquoy, D., Daley, T.J., Hughes, P.D.M., Karofeld, E., 2009. Climate drivers for peatland palaeoclimate records. *Quat. Sci. Rev.* 28, 1811–1819.
- Chylek, P., Folland, C.K., Dijkstra, H.A., Lesins, G., Dubey, M.K., 2011. Ice-core data evidence for a prominent near 20 year time-scale of the Atlantic multidecadal oscillation. *Geophys. Res. Lett.* 38, L13704. <http://dx.doi.org/10.1029/2011GL047501>.
- Compo, G.P., Whitaker, J.S., Sardeshmukh, P.D., Matsui, N., Allan, R.J., Yin, X., Gleason Jr., B.E., Vose, R.S., Rutledge, G., Bessemoulin, P., Brönnimann, S., Brunet, M., Crouthamel, R.I., Grant, A.N., Groisman, P.Y., Jones, P.D., Kruk, M.C., Kruger, A.C., Marshall, G.J., Mauerer, M., Mok, H.Y., Nordli, Ø., Ross, T.F., Trigo, R.M., Wang, X.L., Woodruff, S.D., Worley, S.J., 2011. The twentieth century reanalysis project. *Q. J. R. Meteorol. Soc.* 137, 1–28. <http://dx.doi.org/10.1002/qj.776>.
- Cook, E.R., Peters, K., 1981. The smoothing spline: a new approach to standardizing forest interior tree-ring width series for dendroclimatic studies. *Tree-ring Bull.* 41, 45–53.
- Cook, E.R., Krusic, P.J., 2006. ARSTAN\_41: a Tree-ring Standardization Program Based on Detrending and Autoregressive Time Series Modeling, with Interactive Graphics. Tree-ring Laboratory, Lamont Doherty Earth Observatory of Columbia University, New York.
- Czaja, A., Frankignoul, C., 2002. Observed impact of Atlantic SST anomalies on the North Atlantic oscillation. *J. Clim.* 15, 606–623.
- Currie, R.G., 1995. Luni-solar 18.6- and solar cycle 10–11-year signals in Chinese dryness-wetness indices. *Int. J. Climatol.* 15, 497–515.
- Damon, P.E., Peristykh, A.N., 2000. Radiocarbon calibration and application to geophysics, solar physics, and astrophysics. *Radiocarbon* 42, 137–150.
- Edvardsson, J., Leuschner, H.H., Linderson, H., Linderholm, H.W., Hammarlund, D., 2012a. South Swedish bog pines as indicators of Mid-Holocene climate variability. *Dendrochronologia* 30, 93–103.
- Edvardsson, J., Linderson, H., Rundgren, M., Hammarlund, D., 2012b. Holocene peatland development and hydrological variability inferred from bog-pine dendrochronology and peat stratigraphy – a case study from southern Sweden. *J. Quat. Sci.* 27, 553–563.
- Edvardsson, J., 2013. *Holocene Climate Change and Peatland Dynamics in Southern Sweden Based on Tree-ring Analysis of Subfossil Wood from Peat Deposits*. Lund University. Dissertation.
- Edvardsson, J., Poska, A., Van der Putten, N., Rundgren, M., Linderson, H., Hammarlund, D., 2014. Late-Holocene expansion of a South Swedish peatland and its impact on marginal ecosystems: evidence from dendrochronology, peat stratigraphy and palaeobotanical data. *Holocene* 24, 466–476.
- Edvardsson, J., Rimkus, E., Corona, C., Simanauškiene, R., Kažys, J., Stoffel, M., 2015. Exploring the impact of regional climate and local hydrology on *Pinus sylvestris* L. growth variability – a comparison between pine populations growing on peat soils and mineral soils in Lithuania. *Plant Soil* 392, 345–356.
- Edvardsson, J., Hansson, A., 2015. Multiannual hydrological responses in Scots pine radial growth within raised bogs in southern Sweden. *Silva Fenn.* 49. ISSN 2242–4075.
- Edvardsson, J., Corona, C., Mažeika, J., Pukienė, R., Stoffel, M., 2016. Recent advances in long-term climate and moisture reconstructions from the Baltic region: exploring the potential for a new multi-millennial tree-ring chronology. *Quat. Sci. Rev.* 131, 118–126.
- Esper, J., Krusic, P.J., Peters, K., Frank, D., 2009. Exploration of long-term growth changes using tree-ring detrending program “Spotty”. *Dendrochronologia* 27, 75–82.
- Folland, C.K., Knight, J., Linderholm, H.W., Fereday, D., Ineson, S., Hurrell, J.W., 2009. The summer North Atlantic oscillation: past, present, and future. *J. Clim.* 22, 1082–1103.
- Friedman, J.H., 1984. *A Variable Span Smoother*, Department of Statistics Technical Report LCS 5. Stanford University, Stanford.
- Fritts, H.C., 1976. *Tree Rings and Climate*. Academic Press, London.
- Gastineau, G., Frankignoul, C., 2015. Influence of the North Atlantic SST variability on the atmospheric circulation during the twentieth Century. *J. Clim.* 28, 1396–1416.
- Greatbatch, R.J., 2000. The North Atlantic oscillation. *Stoch. Env. Res. Risk A* 14, 213–242.
- Grinsted, A., Moore, J.C., Jevrejeva, S., 2004. Application of the cross wavelet transform and wavelet coherence to geophysical time series. *Nonlin. Process. Geophys.* 11, 561–566.
- Haigh, J.D., 2000. Solar variability and climate. *Weather* 55, 399–407.
- Haigh, I.D., Eliot, M., Pattiaratchi, C., 2011. Global influences of the 18.61 year nodal cycle and 8.85 year cycle of lunar perigee on high tidal levels. *J. Geophys. Res.* 116, C06025. <http://dx.doi.org/10.1029/2010JC006645>.
- Holmes, R.L., 1983. Computer assisted quality control in tree ring dating and measurement. *Tree-ring Bull.* 43, 69–78.
- Hurrell, J.W., 1995. Decadal trends in the North Atlantic oscillation: regional temperatures and precipitation. *Science* 269, 676–679.
- Hurrell, J.W., Kushnir, Y., Visbeck, M., 2001. The North Atlantic oscillation. *Science* 291, 603–605.
- Jenkins, G.M., Watts, D.G., 1968. *Spectral Analysis and its Applications*. Holden-Day, 525pp.
- Johansson, M., Biman, H., Kahma, K.K., Launiainen, J., 2001. Trends in sea level variability in the Baltic Sea. *Boreal Environ. Res.* 6, 159–179.
- Jones, P.D., Jónsson, T., Wheeler, D., 1997. Extension to the North Atlantic oscillation using early instrumental pressure observations from Gibraltar and South-West Iceland. *Int. J. Climatol.* 17, 1433–1450.
- Justino, F., Peltier, W.R., 2005. The glacial North Atlantic oscillation. *Geophys. Res. Lett.* 32, L21803. <http://dx.doi.org/10.1029/2005GL023822>.
- Keer, R.A., 2000. A North Atlantic climate pacemaker for the centuries. *Science* 288, 1984–1985.
- Kilian, M.R., Van der Plicht, J., Van Geel, B., 1995. Dating raised bogs. New aspects of AMS <sup>14</sup>C wiggle matching, a reservoir effect and climatic change. *Quat. Sci. Rev.* 14, 959–966.
- Knight, J.R., Allan, R.J., Folland, C.K., Vellinga, M., Mann, M.E., 2005. A signature of persistent natural thermohaline circulation cycles in observed climate. *Geophys. Res. Lett.* 32 <http://dx.doi.org/10.1029/2005GL024233>.
- Leuschner, H.H., Sass-Klaassen, U., Jansma, E., Baillie, M.G.L., Spurk, M., 2002. Subfossil European bog oaks: population dynamics and long-term growth depressions as indicators of changes in the Holocene hydro-regime and climate. *Holocene* 12, 695–706.
- Linderholm, H.W., 2001. Climate influence on Scots pine growth on dry and wet soils in the central Scandinavian mountains, interpreted from tree-ring widths. *Silva Fenn.* 35, 415–424.
- Linderholm, H., Moberg, A., Grudd, H., 2002. Peatland pines as climate indicators? A regional comparison of the climatic influence on Scots pine growth in Sweden. *Can. J. For. Res.* 32, 1400–1410.
- Linderholm, M., Jalkanen, R., Salminen, H., Aalto, T., Ogurtsov, M., 2011. The height-increment record of summer temperature extended over the last millennium in Fennoscandia. *Holocene* 21, 319–326.
- Luterbacher, J., Xoplaki, E., Dietrich, D., Jones, P.D., Davies, T.D., Portis, D., Gonzalez-Rouco, J.F., von Storch, H., Gyalistras, D., Casty, C., Wanner, H., 2002. Extending North Atlantic oscillation reconstructions back to 1500. *Atmos. Sci. Lett.* 2, 114–124. <http://dx.doi.org/10.1006/asle.2001.0044>.
- Marcott, S.A., Shakun, J.D., Clark, P.U., Mix, A.C., 2013. A reconstruction of regional and global temperature for the last 11,300 years. *Science* 339, 1198–1201. <http://dx.doi.org/10.1126/science.1228026>.
- Mauquoy, D., van Geel, B., Blaauw, M., Speranza, A., van der Plicht, J., 2004. Changes in solar activity and Holocene climatic shifts derived from <sup>14</sup>C wiggle-match dated peat deposits. *Holocene* 14, 45–52.
- McKinnell, S.M., Crawford, W.R., 2007. The 18.6-year lunar nodal cycle and surface temperature variability in the northeast Pacific. *J. Geophys. Res.* 112, C02002. <http://dx.doi.org/10.1029/2006JC003671>.
- Mellström, A., van der Putten, N., Muscheler, R., de Jong, R., Björck, S., 2015. A shift towards wetter and windier conditions in southern Sweden around the prominent solar minimum 2750 cal a BP. *J. Quat. Sci.* 30, 235–244.
- Mitra, K., Mukherji, S., Dutta, S.N., 1991. Some indications of 18.6 year luni-solar and 10–11 year solar cycles in rainfall in north-west India, the plains of Uttar Pradesh and north-central India. *Int. J. Climatol.* 11, 645–652.
- Moron, V., Vautard, R., Ghil, M., 1998. Trends, interdecadal and interannual oscillations in global sea-surface temperatures. *Clim. Dynam.* 14, 545–569.
- Moss, R.H., Edmonds, J.A., Hibbard, K.A., Manning, M.R., Rose, S.K., van Vuuren, D.P., Carter, T.R., Emori, S., Kainuma, M., Kram, T., Meehl, G.A., Mitchell, J.F.B.,

- Nakicenovic, N., Riahi, K., Smith, S.J., Stouffer, R.J., Thomson, A.M., Weyant, J.P., Wilbanks, T.J., 2010. The next generation of scenarios for climate change research and assessment. *Nature* 463, 747–756.
- Muscheler, R., Beer, J., Kubik, P.W., Synal, H.-A., 2005. Geomagnetic field intensity during the last 60,000 years based on  $^{10}\text{Be}$  and  $^{36}\text{Cl}$  from the Summit ice cores and  $^{14}\text{C}$ . *Quat. Sci. Rev.* 24, 1849–1860. <http://dx.doi.org/10.1016/j.quascirev.2005.1001.1012>.
- Muscheler, R., Joos, F., Beer, J., Müller, S.A., Vonmoos, M., Snowball, I., 2007. Solar activity during the last 1000 yr inferred from radionuclide records. *Quat. Sci. Rev.* 26, 82–97.
- O'Brien, D.P., Currie, R.G., 1993. Observations of the 18.6-year cycle of air pressure and a theoretical model to explain certain aspects of this signal. *Clim. Dynam.* 8, 287–298.
- Olsen, J., Anderson, N.J., Knudsen, M.F., 2012. Variability of the North Atlantic oscillation over the past 5,200 years. *Nat. Geosci.* 5, 808–812. <http://dx.doi.org/10.1038/NGEO1589>.
- Pilcher, J.R., Baillie, M.G.L., Schmidt, B., Becker, B., 1984. A 7272-year tree-ring chronology for Western Europe. *Nature* 312, 150–152.
- Raspopov, O.M., Dergachev, V.A., Kolström, T., 2004. Periodicity of climate conditions and solar variability derived from dendrochronological and other palaeoclimatic data in high latitudes. *Palaeogeogr. Palaeoclimatol.* 209, 127–139.
- Ray, R.D., 2006. Decadal climate variability: Is there a tidal connection? *J. Clim.* 20, 3542–3560. <http://dx.doi.org/10.1175/JCLI4193.1>.
- Rayner, N.A., Parker, D.E., Horton, E.B., Folland, C.K., Alexander, L.V., Rowell, D.P., Kent, E.C., Kaplan, A., 2003. Global analyses of sea surface temperature, sea ice, and night marine air temperature since the late nineteenth century. *J. Geophys. Res.* 108, 4407. <http://dx.doi.org/10.1029/2002JD002670>.
- Rögnvaldsson, Ö.E., 1993. Spectral Estimation using the Multi-taper Method. Science Institute, University of Iceland, p. 36. Report RH-13-93.
- Stoffel, M., Khodri, M., Corona, C., Guillet, S., Poulain, V., Bekki, S., Guiot, J., Luckman, B.H., Oppenheimer, C., Lebas, N., Beniston, M., Masson-Delmotte, V., 2015. Estimates of volcanic-induced cooling in the Northern Hemisphere over the past 1,500 years. *Nat. Geosci.* <http://dx.doi.org/10.1038/NGEO2526>.
- Stoica, P., Moses, R., 2005. *SPectral Analysis of Signals*. Prentice Hall, Inc., Upper Saddle River, New Jersey.
- Sutton, R.T., Allen, M.R., 1997. Decadal predictability of North Atlantic sea surface temperature and climate. *Nature* 388, 563–567.
- Sutton, R.T., Hodson, D.L.R., 2005. Atlantic Ocean forcing of North American and European summer climate. *Science* 309, 115–118.
- Sutton, R.T., Dong, B., 2012. Atlantic Ocean influence on a shift in European climate in the 1990s. *Nat. Geosci.* 5 <http://dx.doi.org/10.1038/NGEO1595>.
- Thomson, D.J., 1982. Spectrum estimation and harmonic analysis. *Proc. IEEE* 70, 1055–1096.
- Torrence, C., Compo, G.P., 1998. A practical guide to wavelet analysis. *B. Am. Meteorol. Soc.* 79, 61–78.
- van Loon, H., Rodgers, J.C., 1978. The seesaw in winter temperatures between Greenland and Northern Europe. Part I: general description. *Mon. Weather Rev.* 106, 296–310.
- van Oldenborgh, G.J., te Raa, L.A., Dijkstra, H.A., Philip, S.Y., 2009. Frequency- or amplitude-dependent effects of the Atlantic meridional overturning on the tropical Pacific Ocean. *Ocean. Sci.* 5, 293–301. <http://dx.doi.org/10.5194/os-5-293-2009>.
- Waddington, J.M., Morris, P.J., Kettridge, N., Granath, G., Thompson, D.K., Moore, P.A., 2014. Hydrological feedbacks in northern peatlands. *Ecohydrology*. <http://dx.doi.org/10.1002/eco.1493>.
- Wanner, H., Beer, J., Butikofer, J., Crowley, T.J., Cubasch, U., Flückiger, J., Goussé, H., Grosjean, M., Joos, F., Kaplan, J.O., Kuttel, M., Müller, S.A., Prentice, O.C., Solomina, O., Stocker, T.F., Tarasov, P., Wagner, M., Widmann, M., 2008. Mid- to Late Holocene climate change: an overview. *Quat. Sci. Rev.* 27, 1791–1828.
- Wei, W., Lohmann, G., 2012. Simulated Atlantic multidecadal oscillation during the Holocene. *J. Clim.* 25, 6989–7002. <http://dx.doi.org/10.1175/JCLI-D-11-00667.1>.
- Wigley, T.M.L., Briffa, K.R., Jones, P.D., 1984. On the average of correlated time series, with applications in dendroclimatology and hydrometeorology. *J. Clim. Appl. Meteorol.* 23, 201–213.
- Woodhouse, C.A., Gille, E.P., Overpeck, J.T., Karl, T.R., Guttman, N.B., 1998. New database for North American paleodrought. *Earth Syst. Monit.* 8, 1–6.
- Wu, W., Geller, M.A., Dickinson, R.E., 2002. The response of soil moisture to long-term variability of precipitation. *J. Hydrometeorol.* 3, 604–613.
- Yndestad, H., 2006. The influence of the lunar nodal cycle on Arctic climate. *ICES J. Mar. Sci.* 63, 401–420.
- Yndestad, H., Turrell, W.R., Ozhigin, V., 2008. Lunar nodal tide effects on variability of sea level, temperature, and salinity in the Faroe-Shetland channel and the Barents Sea. *Deep Sea Res. Part I Oceanogr. Res. Pap.* 55, 1201–1217.